

1 **Conservation and Convergence of Genetic Architecture in** 2 **the Adaptive Radiation of *Anolis* lizards**

3
4 **Joel W. McGlothlin,^{1,*} Megan E. Kobiela,² Helen V. Wright,³ Jason J. Kolbe,⁴ Jonathan B.**
5 **Losos,⁵ and Edmund D. Brodie III⁶**

6
7 1. Department of Biological Sciences, Virginia Tech, Blacksburg, Virginia 24061; email:
8 joelmcg@vt.edu

9 2. School of Biological Sciences, University of Nebraska, Lincoln, Nebraska 68588; email:
10 mkobiela2@unl.edu

11 3. Computing Community Consortium, Computing Research Association, Washington, DC
12 20036; email: helenvwright2@gmail.com

13 4. Department of Biological Sciences, University of Rhode Island, Kingston, Rhode Island
14 02881; email: jjkolbe@uri.edu

15 5. Department of Biology, Washington University, Saint Louis, Missouri 63130; email:
16 losos@wustl.edu

17 6. Department of Biology and Mountain Lake Biological Station, University of Virginia,
18 Charlottesville, Virginia 22904; email: edb9j@virginia.edu

19 * Corresponding author

20
21 Short running title: *Conservation and Convergence of G*

22 ABSTRACT: The **G** matrix, which quantifies the genetic architecture of traits, is often viewed as an
23 evolutionary constraint. However, **G** can evolve in response to selection and may also be viewed
24 as a product of adaptive evolution. The evolution of similar **G** matrices in similar environments
25 would suggest that **G** evolves adaptively, but it is difficult to disentangle such effects from
26 phylogeny. Here, we use the adaptive radiation of *Anolis* lizards to ask whether convergence of **G**
27 accompanies the repeated evolution of habitat specialists, or ecomorphs, across the Greater
28 Antilles. We measured **G** in seven species representing three ecomorphs (trunk-crown, trunk-
29 ground, and grass-bush). We found that the overall structure of **G** does not converge. Instead, the
30 structure of **G** is well conserved and displays a phylogenetic signal. However, several elements of
31 **G** showed signatures of convergence, indicating that some aspects of genetic architecture have
32 been shaped by selection. Most notably, genetic correlations between limb traits and body traits
33 were weaker in long-legged trunk-ground species, suggesting effects of recurrent selection on
34 limb length. Our results demonstrate that common selection pressures may have subtle but
35 consistent effects on the evolution of **G**, even as the overall pattern of genetic architecture
36 remains conserved.

37

38 *Keywords:* adaptive radiation, *Anolis* lizards, constraint, **G** matrix, genetic correlation,
39 quantitative genetics

40 **Introduction**

41 Genetic variation translates natural selection into evolutionary change (Falconer and MacKay
42 1996; Roff 1997). Understanding the nature of such genetic variation and the processes that shape
43 it has been a goal of evolutionary biology since the early days of population genetics
44 (Dobzhansky 1937). In evolutionary quantitative genetics, the pattern of genetic variation in a
45 population is described by the genetic variance-covariance matrix \mathbf{G} , which predicts the
46 multivariate response to phenotypic selection (Lande 1979). The \mathbf{G} matrix can be used to make
47 accurate predictions of short-term evolutionary change (Grant and Grant 1995), but its utility for
48 making long-term predictions is more suspect because \mathbf{G} itself may evolve during adaptive
49 evolution (Turelli 1988; Stepan et al. 2002). Although early theory argued for the stability of \mathbf{G}
50 (Lande 1980), both more recent theoretical (Agrawal et al. 2001; Jones et al. 2003; 2004, 2012,
51 2014; Revell 2007; Arnold et al. 2008) and empirical results (Stepan et al. 2002; Cano et al.
52 2004; Doroszuk et al. 2008; Hine et al. 2009; Eroukhmanoff and Svensson 2011; Björklund et al.
53 2013; Careau et al. 2015) suggest that \mathbf{G} can and does evolve, sometimes rapidly. Given enough
54 time, selection is expected to align \mathbf{G} with the adaptive landscape (Cheverud 1984; Arnold et al.
55 2001, 2008; Jones et al. 2003, 2014; Revell 2007), potentially making \mathbf{G} as much as a product of
56 adaptive evolution as a constraint upon it (Merilä and Björklund 2004).

57 Because stability and evolutionary lability of \mathbf{G} are both plausible theoretical outcomes,
58 the relative importance of history and adaptation in shaping \mathbf{G} is largely an empirical question
59 (Arnold et al. 2008). Several studies have shown a relationship between the shape of \mathbf{G} and
60 divergence, suggesting the importance of genetic constraints in channeling evolutionary
61 outcomes (Bégin and Roff 2003; 2004; Blows and Hoffmann 2005; McGuigan et al. 2005;

62 McGuigan 2006; Hansen and Houle 2008; Walsh and Blows 2009; Chenoweth et al. 2010;
63 Bolstad et al. 2014; Houle et al. 2017; McGlothlin et al. 2018; Walter et al. 2018). The early
64 stages of adaptive radiation are expected to be aligned with the “genetic line of least resistance”
65 describing the direction of greatest genetic variation within a population (Schluter 1996).
66 Although natural selection should be able to push phenotypes away from this line given enough
67 time, recent results suggest that evolutionary change may be predicted by axes of genetic
68 variation for tens of millions of years (Houle et al. 2017; McGlothlin et al. 2018). Conversely, it
69 is well established that both directional and nonlinear selection may alter aspects of **G**. For
70 example, correlational selection, which occurs when certain combinations of traits are favored
71 over others, can directly alter the strength of genetic correlations each generation (Phillips and
72 Arnold 1989; Jones et al. 2003; Revell 2007). Patterns of genetic correlation are often congruent
73 with axes of correlational selection in the wild (Brodie 1989; 1992; McGlothlin et al. 2005; Roff
74 and Fairbairn 2012), and genetic correlations can evolve in response to artificial correlational
75 selection (Delph et al. 2011; Steven et al. 2020).

76 Although comparative studies of **G** have become more common in recent years (Steppan
77 et al. 2002; Bégin and Roff 2003; Hine et al. 2009; Eroukhmanoff and Svensson 2011; Walter et
78 al. 2018), none have been able to disentangle the effects of shared ancestry from similar selection
79 pressures in determining the evolution of **G**. Convergent evolution of **G** or its elements in similar
80 environments would provide strong evidence that changes in **G** represent adaptation of genetic
81 architecture (Losos 2011). The adaptive radiation of West Indian *Anolis* lizards provides an ideal
82 testing ground for hypotheses about the evolution of **G** because the effects of phylogenetic
83 history and ecological selection are largely decoupled (Losos 1994; 2009; 2011). In the Greater
84 Antilles, anoles have diversified into 120 species, 95 of which can be classified as one of six

85 habitat specialists, or ecomorphs, each of which has evolved multiple times throughout the *Anolis*
86 radiation (Williams 1972; Losos et al. 1998; Beuttell and Losos 1999; Losos 2009). Species with
87 dissimilar morphology on the same island tend to be more closely related than are those with
88 similar morphology on different islands, indicating that the characteristic morphology of
89 ecomorphs is due to convergent evolution (Losos et al. 1998; Harmon et al. 2005; Mahler et al.
90 2013). This repeated adaptive radiation leads to explicit predictions for the evolution of **G**. If **G**
91 responds predictably to similar selection pressures, **G** should show signatures of convergence
92 among the independent origins of the same ecomorph. Conversely, if **G** evolves relatively slowly
93 and does not respond predictably to similar selection pressures, **G** or its elements should be more
94 similar within lineages than within ecomorph classes.

95 Previous work in *Anolis* using phenotypic variance-covariance matrices (**P**) as proxies for
96 **G** (Cheverud 1988) suggests that selection may indeed lead to convergence in (co)variance
97 structure. A study comparing **P** in eight *Anolis* species showed significant variation in covariance
98 structure across the radiation and demonstrated convergent changes in **P** in three distantly related
99 species from the same ecomorph class (Kolbe et al. 2011). In a separate study, **P** showed
100 significant alignment with the matrix of nonlinear selection (γ) in *A. cristatellus*, suggesting that
101 contemporary stabilizing and correlational selection may act to shape the pattern of phenotypic
102 (co)variance within species (Revell et al. 2010). These results suggest that selection plays a role
103 in shaping genetic architecture in anoles, but patterns of phenotypic covariance do not necessarily
104 mirror patterns of genetic covariance (Hadfield et al. 2007). Thus, comparative studies that
105 directly estimate **G** are necessary to test whether its structure is more influenced by phylogenetic
106 history or convergent evolution.

107 In this study, we compare **G** matrices in seven *Anolis* species reared in a controlled
108 laboratory environment. We chose species from lineages originating on three different islands,
109 Puerto Rico, Jamaica, and Cuba, and included three ecomorphs, trunk-crown (three species),
110 trunk-ground (three species), and grass-bush (one species), which are distinguished by their
111 habitat use, coloration, and skeletal morphology (Williams 1972; Beuttell and Losos 1999;
112 Harmon et al. 2005; Losos 2009). Trunk-crown lizards are typically found high in trees and are
113 usually green with relatively short legs for climbing and clinging to narrow perches. Trunk-
114 ground lizards tend to be found on low perches or on the ground and are typically brown with
115 long hindlimbs that aid in running quickly and jumping far (Losos and Sinervo 1989; Losos
116 1990; Irschick and Losos 1998; Beuttell and Losos 1999). The third ecomorph, grass-bush, has a
117 slender body that matches its narrow perches and long hindlimbs that allow it to both run and
118 jump well (Losos 1990; Beuttell and Losos 1999). The three trunk-crown species are distantly
119 related to one another, as are the trunk-ground species. Both ecomorphs may have evolved three
120 separate times, although it cannot be ruled out that one of these ecomorphs represents the
121 ancestral state for the anole radiation (Losos 2009). Because of the importance of skeletal
122 morphology, and limb length in particular, to the evolution of these ecomorphs, our estimates of
123 **G** focus on skeletal traits.

124 Our previous results have shown that **G** varies substantially across these *Anolis* species,
125 while retaining conserved axes of genetic variation (McGlothlin et al. 2018). Specifically, **G**
126 matrices varied most in size (overall genetic variance), and the major axis of genetic variance
127 remained similar in orientation across all species. This major axis of genetic variance was similar
128 in orientation to the major axis of morphological divergence, suggesting that divergence has
129 occurred along a genetic line of least resistance even though **G** has not remained constant. The

130 largest evolutionary changes in \mathbf{G} were also aligned with the major axes of both genetic variance
131 and morphological divergence. This triple alignment may have been caused by deep genetic
132 constraints underlying both the evolution of \mathbf{G} and morphological divergence, alignment of \mathbf{G}
133 with the adaptive landscape, genetic drift, or some combination of the three (McGlothlin et al.
134 2018).

135 Here, we explicitly consider the role of selection in shaping \mathbf{G} -matrix evolution across the
136 *Anolis* radiation by testing whether aspects of \mathbf{G} show patterns of convergence that mirror the
137 repeated evolution of ecomorphs. To do so, we use two types of comparisons. First, we test for
138 convergence of the overall structure of \mathbf{G} by asking whether random skewers correlations, which
139 are estimates of pairwise similarity in the predicted multivariate response to selection, are better
140 predicted by shared evolutionary history or shared ecology. Second, we conduct similar tests for
141 individual elements of \mathbf{G} (i.e., variances and covariances of individual traits) to test for signatures
142 of convergence on a finer scale. Although many processes, including both selection and drift,
143 could lead to similarities in \mathbf{G} among more closely related species, convergence in the structure
144 of \mathbf{G} among distantly related species of the same ecomorph would provide strong evidence that \mathbf{G}
145 may be predictably shaped by common selection pressures.

146

147

148

Methods

149

Estimation of \mathbf{G}

150 Detailed methods for estimation of the \mathbf{G} matrices used here are reported elsewhere (McGlothlin
151 et al. 2018). Briefly, adults from seven *Anolis* species, representing independent origins of trunk-

152 crown (*A. evermanni*, Puerto Rico; *A. grahmi*, Jamaica; *A. smaragdinus*, a Bahamian species
153 descended from *A. porcatus* on Cuba), trunk-ground (*A. cristatellus*, Puerto Rico; *A. lineatopus*,
154 Jamaica; *A. sagrei*, Cuba), and grass-bush ecomorphs (*A. pulchellus*, Puerto Rico), were collected
155 from the wild (Fig. 1). Due to travel restrictions, species from Cuban lineages were collected
156 from South Bimini, The Bahamas, where they occur naturally. These seven species shared a
157 common ancestor approximately 41.5–43.5 million years ago, and the most recent phylogenetic
158 split (between *A. cristatellus* and *A. pulchellus*) dates is estimated at 19.8–22.5 million years ago
159 (fig. 1, Zheng and Wiens 2016; Poe et al. 2017).

160 Adults were housed in individual cages in the laboratory except when paired for breeding
161 and held at controlled photoperiod (12L:12D for Puerto Rican and Jamaican adults and 13L:11D
162 for Bahamian adults), temperature (28°C during the day and 25°C at night), and relative humidity
163 (65%). Lizards were provided with a perch, a mesh hammock for basking near an adjacent UVB
164 bulb, and a carpet substrate. Adults were mated in a paternal half-sib breeding design (average of
165 47 sires and 69 dams per species) to produce offspring (2,904 total, see McGlothlin et al. 2018
166 for more sampling details). Laying females were provided with potted plants, which were
167 checked weekly for eggs, which were placed in individual cups with a 1:1 mixture of water and
168 vermiculite and held in an incubator at 28°C and 80% humidity until hatching.

169 Juveniles were reared in individual cages until 6 months of age and were provided with
170 crickets and water daily. At 0, 1, 3, and 6 months of age, we X-rayed juveniles by chilling them
171 for 10 min at 5°C in small plastic bags. The bags were then secured with masking tape to a film
172 cartridge (Kodak Biomax XAR) for imaging in a Faxitron 43805N radiography system.
173 Developed radiographs were digitized using a flatbed scanner. Using ImageJ (NIH), we measured
174 snout-vent length (SVL) and eight other skeletal traits, jaw length (JL), head width (HW),

175 pectoral width (PECT), pelvis width (PELV), humerus (HUM), ulna (UL), femur (FEM), and
176 tibia (TIB; see Fig. 1A for location of measured traits). In all, 9,369 individual X-ray images
177 were measured (McGlothlin et al. 2018). We used multivariate repeated measures animal models
178 in ASReml 3.0 (Gilmour et al. 2009) to estimate **G** matrices for natural-log transformed traits,
179 with size (natural-log SVL) as a covariate to correct for age and growth. These models included
180 two random animal effects, one linked to the pedigree to estimate additive genetic (co)variance
181 and a second unlinked effect to estimate effects of permanent environment. All species could not
182 be reliably sexed as juveniles; therefore, we did not correct for sex in our models. In one species
183 that has been studied extensively in the laboratory, *A. sagrei*, sexual size dimorphism is not
184 noticeable at hatching and only becomes elaborated after 6 months of age with the maturation of
185 testes in males (Cox et al. 2017). Genetic correlations are shown (along with heritabilities) in
186 table A1 and visualized in fig. 1; full **G** matrices, reprinted from McGlothlin et al. (2018), are
187 also shown in table A1. Permanent environment (co)variances, which were generally at least an
188 order of magnitude smaller than genetic (co)variances, and residual (co)variances are not
189 presented here but were used in the calculation of total phenotypic variance for calculating
190 heritabilities. As reported previously, in all but two species, all eight traits we measured were
191 significantly heritable (mean h^2 across species \pm s.d.: JL, $.40 \pm .150$; HW, $.22 \pm .084$; PECT, $.21$
192 $\pm .073$; PELV, $.22 \pm .046$; HUM, $.16 \pm .047$; UL, $.15 \pm .042$; FEM, $.45 \pm .143$, TIB, $.54 \pm .091$,
193 table A1; McGlothlin et al. 2018). In general, genetic correlations were strong and positive for
194 pairs of limb traits and both weaker and more variable across species for other trait combinations
195 (fig. 1, table A1; McGlothlin et al. 2018).

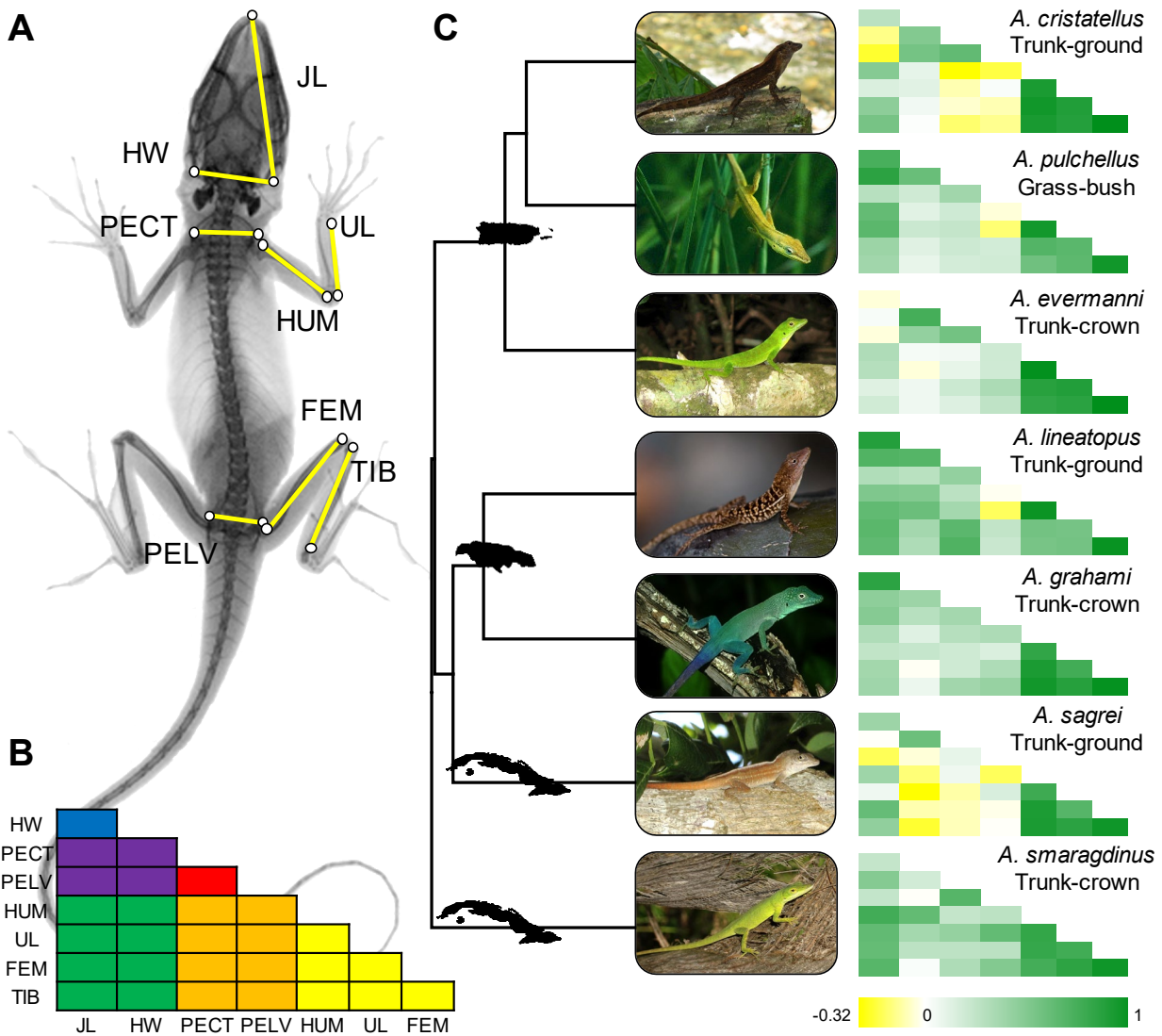


Figure 1: (A) Traits measured in this study: JL = jaw length, HW = head width, PECT = pectoral width, PELV = pelvis width, HUM = humerus, UL = ulna, FEM = femur, TIB = tibia. (B) Schematic of a genetic correlation matrix showing the location of each trait. Elements are color-coded based on morphological modules (head, body, and limbs; see Methods), showing within-module correlations in primary colors (blue = head, red = body, yellow = limbs) and between module correlations in secondary colors (violet = head-body, green = head-limb, orange = body-limb). (C) Graphical representation of genetic correlation matrices for each species. Positive correlations are shown in green and negative correlations are shown in yellow, with brighter colors signifying stronger correlations. See table A1 for values. Photographs by J.B.L. (*A. pulchellus*, *A. lineatopus*, and *A. grahami*), and E.D.B. III (all other species).

196

Statistical Analyses

197 All statistical analyses using \mathbf{G} matrices were performed in R 3.5.3 (R Core Team 2019). To
198 incorporate estimation error in \mathbf{G} into our analyses, we used the restricted maximum-likelihood
199 multivariate normal (REML-MVN) method developed by Houle and Meyer (2015). We used
200 point estimates of \mathbf{G} and the sampling (co)variance matrix of (co)variance components, which is
201 calculated by ASReml as the inverse of the average information matrix (Gilmour et al. 2009), to
202 define a multivariate normal distribution. From this distribution, we generated 10,000 samples of
203 \mathbf{G} for each species using the function *rmvn* from the R package *mgcv* (Wood 2012). All further
204 analyses were run using both the point estimates of \mathbf{G} , from which we estimated parameters and
205 test statistics, and the set of 10,000 REML-MVN samples per species, from which we calculated
206 95% confidence intervals using the 2.5% and 97.5% quantiles from the parameter distribution. A
207 parameter was considered to be statistically supported when its 95% confidence interval did not
208 overlap the expected null value (often zero). We clarify the specific ways REML-MVN samples
209 were used for each analysis below.

210 To quantify pairwise similarity in the overall structure of \mathbf{G} , we used random skewers
211 analysis, which compares the response to selection predicted by a pair of \mathbf{G} matrices (Marroig
212 and Cheverud 2001; Cheverud and Marroig 2007; Revell 2007; Aguirre et al. 2014). Random
213 skewers analysis has the advantage of providing an evolutionarily relevant comparison of \mathbf{G}
214 using a single metric. We used the function *RandomSkewers* in the R package *evolQG* (Melo et
215 al. 2015) to apply 10,000 random selection gradients (β) to all seven \mathbf{G} matrices. Each element of
216 these skewers was drawn from a normal distribution, after which each skewer was normalized to
217 unit length and used to calculate the predicted multivariate selection response ($\Delta\bar{z}$) from the

218 multivariate breeder's equation, $\Delta\bar{\mathbf{z}} = \mathbf{G}\boldsymbol{\beta}$ (Lande 1979). The correlation in response to selection
219 for two species, or the random skewers correlation (r_{RS}), was calculated as the pairwise vector
220 correlation of the resultant 10,000 estimates of $\Delta\bar{\mathbf{z}}$. To incorporate estimation error, r_{RS} was
221 recalculated for 10,000 sets of seven \mathbf{G} matrices each using our REML-MVN samples. We report
222 the mean and 95% confidence intervals of this distribution in addition to our point estimate.
223 Incorporating error pairs of \mathbf{G} matrices leads to negatively skewed distributions of the REML-
224 MVN estimates of r_{RS} . Thus, means of the REML-MVN estimates of r_{RS} tend to be lower than
225 the point estimates.

226 To determine whether more closely related species had more similar \mathbf{G} matrices, we used
227 a Mantel test to compare a matrix of r_{RS} to a patristic distance matrix, which was calculated using
228 a tree pruned from a dated squamate phylogeny (Zheng and Wiens 2016); dates from a tree of all
229 *Anolis* species (Poe et al. 2017), which had identical topology for our species, were similar.
230 Although Mantel tests are not useful for comparing (co)variance matrices directly (Steppan et al.
231 2002) and are not recommended for use in the phylogenetic comparative method when they can
232 be avoided, they are the only option when comparative analyses involve data that can only be
233 expressed as either a correlation or a distance between species (Harmon and Glor 2010). A
234 negative Mantel correlation ($r_M < 0$) between r_{RS} and patristic distance would indicate that the
235 similarity in the structure of \mathbf{G} is explained by phylogenetic similarity. To determine whether
236 unrelated species of the same ecomorph displayed convergence in the structure of \mathbf{G} , we
237 generated a matrix consisting of zeros (different ecomorph) and ones (same ecomorph) and
238 compared it to a matrix of r_{RS} using a partial Mantel test that used the patristic distance matrix as
239 the control matrix. The single grass-bush species, *A. pulchellus*, was excluded from this and all

240 other analyses that included an ecomorph effect. A positive correlation ($r_M < 0$) between the r_{RS}
241 matrix and the ecomorph matrix would indicate convergence.

242 Mantel correlations were calculated in R using the base function `corr` (simple Mantel test)
243 or the function `pcor` (partial Mantel test) from the package `ppcor` (Kim 2015). We did not perform
244 permutation tests to assess statistical significance as is the typical practice when performing
245 Mantel tests. Rather, we conducted separate Mantel tests for each of 10,000 sets of r_{RS} matrices
246 calculated using our REML-MVN samples and report the mean and 95% confidence intervals of
247 this distribution.

248 Evolutionary patterns in \mathbf{G} may involve changes that are subtler than can be detected in
249 analyses of its overall structure. Therefore, we also tested for the effects of shared evolutionary
250 history and shared ecology on the individual elements of \mathbf{G} . We compared genetic variances
251 (diagonal elements of \mathbf{G}) and genetic correlations (off-diagonal elements of \mathbf{G} standardized by
252 the square root of the product of the variances) across \mathbf{G} matrices, testing for both phylogenetic
253 signal and differences between ecomorphs (trunk-crown vs. trunk-ground). We present
254 comparisons of genetic correlations rather than genetic covariances so that tests for associations
255 between traits would be independent of differences in variance across species. However, we note
256 that analyses using covariances gave nearly identical results (not shown).

257 To test for the effects of shared evolutionary history, we used Blomberg's K as an
258 estimate of phylogenetic signal (Blomberg et al. 2003; implemented in the R package `phytools`,
259 Revell 2012). Values of $K = 1$ indicate phylogenetic signal consistent with a Brownian motion
260 model of evolution. Values of $K < 1$ indicate weaker phylogenetic signal, and $K > 1$ indicate
261 stronger signal than would be predicted from a Brownian motion model. We tested for effects of
262 shared ecology on genetic variance and genetic correlations using phylogenetic generalized least

263 squares (Martins and Hansen 1997) with ecomorph as a predictor (coding trunk-crown as 0 and
264 trunk-ground as 1; *A. pulchellus* was excluded), our dated tree, and an assumption of Brownian
265 motion evolution (implemented in the R package APE, Paradis et al. 2004). Alternative models
266 that assumed an Ornstein-Uhlenbeck evolutionary model provided similar results (not shown).
267 For each test, we report the evolutionary correlation (r_e) between the element of \mathbf{G} and ecomorph
268 to remove effects of scale. For a given element of \mathbf{G} , $r_e > 0$ indicates a larger value for trunk-
269 ground species, and $r_e < 0$ indicates a larger value for trunk-crown species. Both of these analyses
270 were conducted for both our point estimates and our REML-MVN samples to incorporate
271 estimation error. Using the 95% confidence intervals from the distributions of REML-MVN
272 estimates, we note deviations from both $K = 0$ and $K = 1$ for phylogenetic signal and $r_e = 0$ for the
273 evolutionary correlation.

274 For visualization, we grouped our estimates of phylogenetic signal and evolutionary
275 correlation into six groups based on phenotypic module. Three groups consisted of elements of \mathbf{G}
276 within modules, head (JW, HL), body (PECT, PELV), and limbs (HUM, UL, FEM, and TIB),
277 and three contained elements of \mathbf{G} between modules, head-limb, head-body, and body-limb.

278

279

280

Results

281

Overall Structure of \mathbf{G}

282

283

284

Predicted responses to selection were highly correlated between all pairs of species (mean $r_{RS} =$
.84, range .75 – .92, REML-MVN mean $r_{RS} = 0.73$, range 0.61 – 0.86; table A2, fig. 2),
suggesting that the species have \mathbf{G} matrices with similar overall structure despite being separated

285 for 20–44 million years. **G**-matrix similarity was negatively correlated with phylogenetic distance
286 ($r_M = -.44$; REML-MVN estimate: r_M [95% CI] = $-.41$ [$-.59, -.15$]), indicating that closely related
287 species have **G** matrices that predict a more similar evolutionary response. More distantly related
288 pairs of species also displayed more variable values of r_{RS} , with some distantly related pairs of
289 species showing highly similar **G** matrices and others showing highly dissimilar **G** (fig. 2).
290 Overall similarity of **G** was not predicted by ecomorph ($r_M = -.12$; REML-MVN estimate: r_M
291 [95% CI] = $.04$ [$-.22, .32$]). However, the two distantly related trunk-ground species *A.*
292 *cratatellus* and *A. sagrei* did have highly similar **G** matrices (figs. 2 & 3).

293

294 *Individual Elements of G*

295 All individual elements of **G** showed phylogenetic signal significantly higher than $K = 0$ but
296 indistinguishable from $K = 1$, which is the null expectation of the Brownian motion model (mean
297 $K = .91$, REML-MVN mean $K = .94$; fig. 4A, table A3). Phylogenetic signal did not exhibit any
298 detectable patterns across trait groups (fig. 4A).

299 Six elements of **G** differed significantly between trunk-crown and trunk-ground
300 ecomorphs. Specifically, genetic correlations between pelvis width and both jaw length and all
301 four limb bones were significantly lower in trunk-ground species than in trunk-crown species
302 (fig. 4B; table A4). In addition, genetic correlations between jaw length and femur length were
303 higher in trunk-ground species than in trunk-crown species (fig. 4B; table A4). In some cases,
304 these effects involved changes in the sign of genetic correlations from positive in trunk-crown
305 species to negative in trunk-ground species (fig. 1). Although not a statistically significant effect,
306 genetic correlations both among limb bones and between pectoral width and all four limb bones

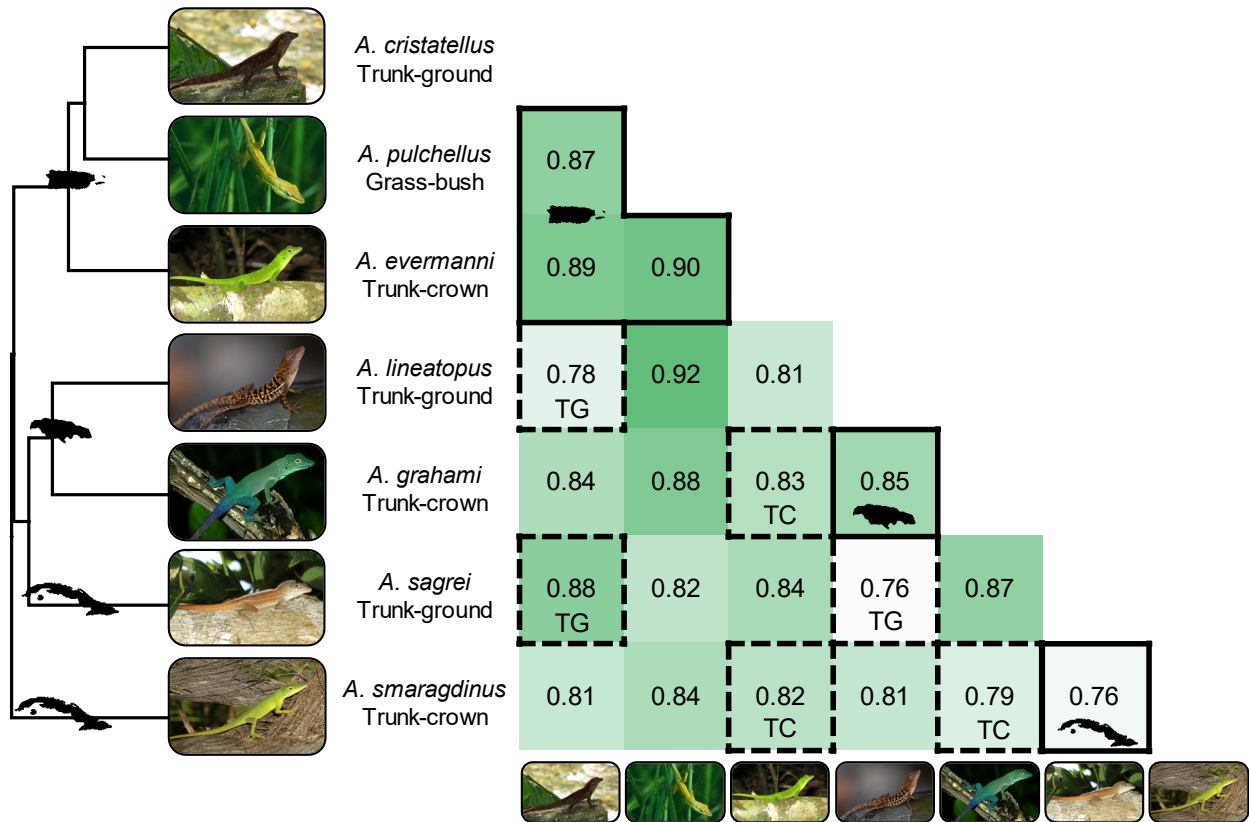


Figure 2: Correlations between species in the overall structure of the **G** matrix as measured via random skewers correlations (r_{RS}). Stronger correlations are represented by darker shading. Within-island comparisons are shown with a solid border, and within-ecomorph comparisons are shown with a dashed border (TC = trunk-crown, TG = trunk-ground). Islands of origin are represented by their shapes on the phylogeny (Puerto Rico, Jamaica, and Cuba, from top to bottom) and for the three within-island comparisons. Note that despite originating on Cuba, *A. sagrei* is actually more closely related to Jamaican species than to *A. smaragdinus*. The phylogeny is pruned from a dated tree of squamates (Zheng and Wiens 2016).

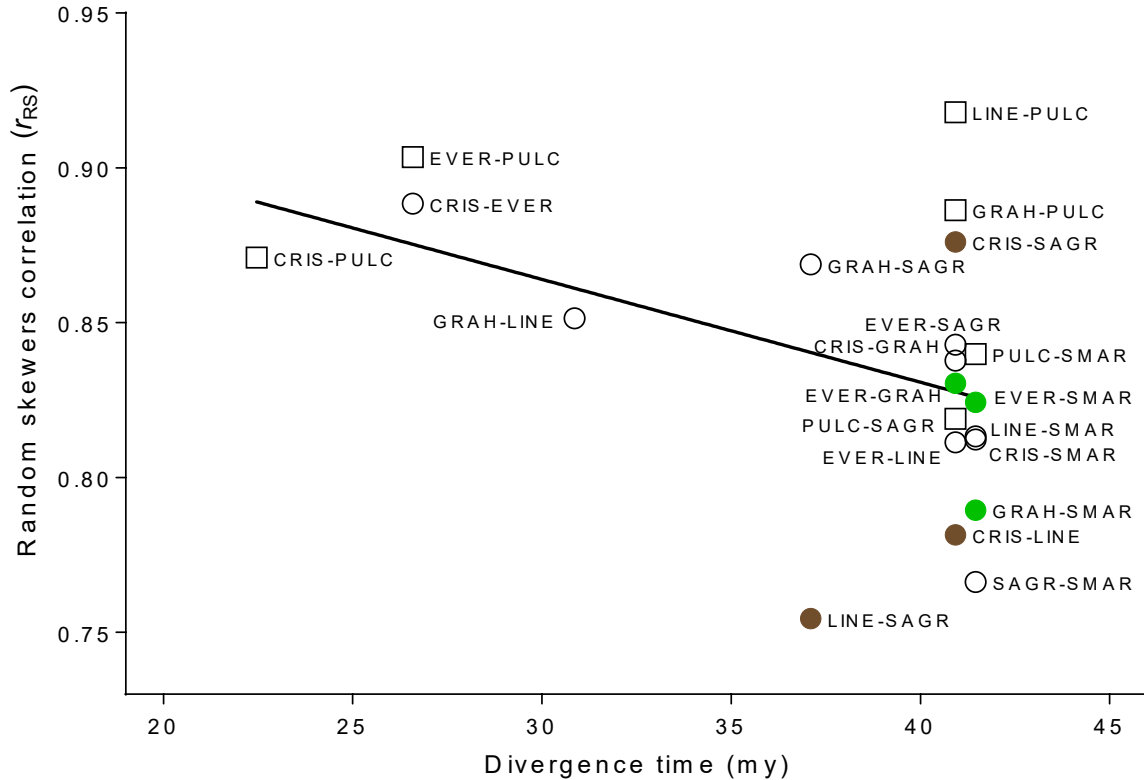


Figure 3: Relationship between divergence time (millions of years, my) and random skewers correlations (r_{RS}). **G** matrices of more distantly related species are significantly less similar and more variable in r_{RS} . Within-ecomorph comparisons are shown as colored circles (green = trunk-crown and brown = trunk-ground), with trunk-crown/trunk-ground comparisons as open circles and comparisons with the grass-bush species as open squares. Each point is labeled with four letter codes for the two species under comparison (CRIS = *A. cristatellus*, EVER = *A. evermanni*, GRAH = *A. grahami*, LINE = *A. lineatopus*, PULC = *A. pulchellus*, SAGR = *A. sagrei*, SMAR = *A. smaragdinus*). A line of best fit from a least-squares regression is added for visualization.

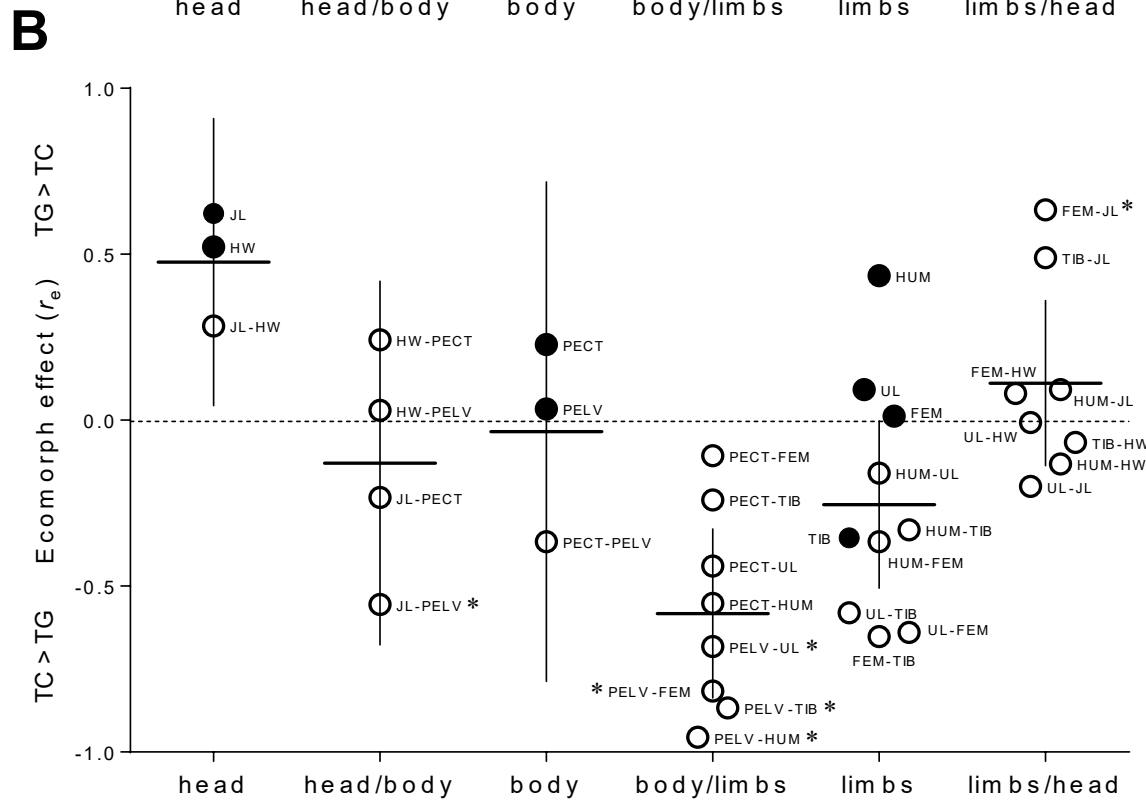
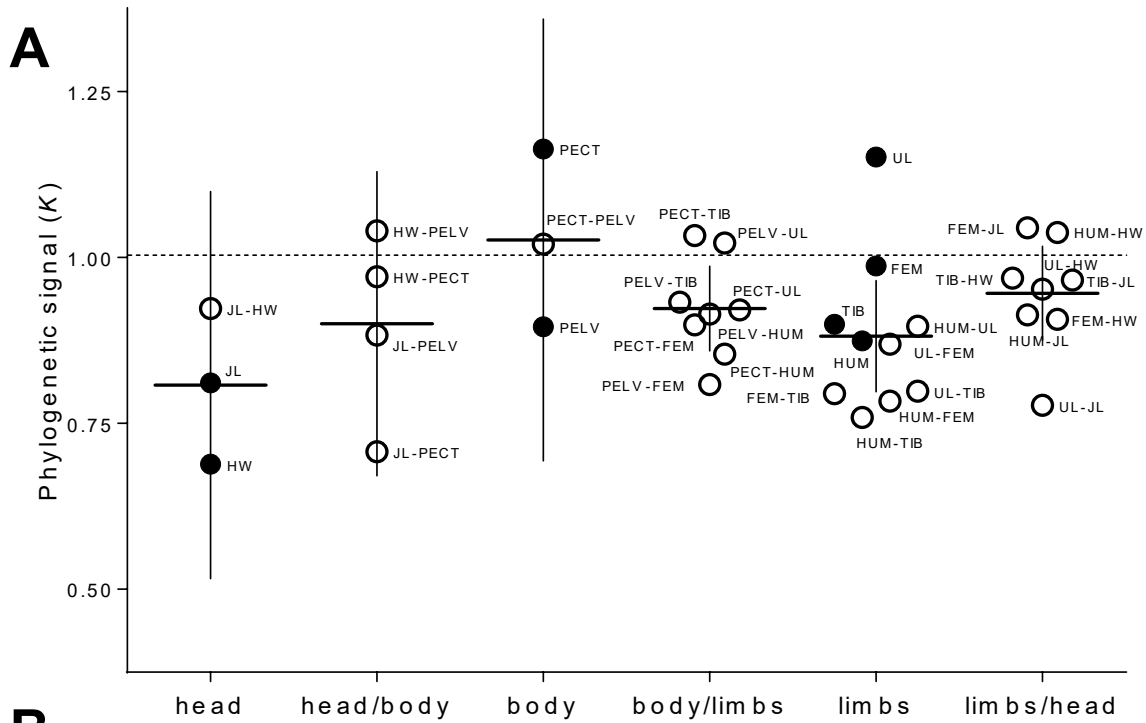


Figure 4 (previous page): Element-by-element comparisons of genetic variances (solid circles) and correlations (open circles). Elements are split into three within-module groups (head, body, and limbs) and three between-module groups (head/body, body/limb, and limb/head) and are labeled with abbreviations as in Fig. 1. Bars show means and 95% confidence intervals for a set of point estimates within a group and are presented for visualization purposes only. (A) Strength of phylogenetic signal, as estimated using Blomberg's K . Estimates were clustered around $K = 1$, suggesting phylogenetic signal consistent with Brownian motion. (B) Ecomorph effects from phylogenetic least squares, given as the evolutionary correlation (r_e). Points above the midline indicate that trunk-ground species had higher values of a given element of \mathbf{G} than did trunk-crown species; the converse is true below the midline. Six genetic correlations showed a significant correlation with ecomorph (trunk-ground vs. trunk-crown; $p < .05$, denoted by *).

307 tended to be weaker in trunk-ground species than in trunk-crown species, indicating a trend
308 toward weaker integration among limb and body traits in trunk-ground species.

309 Although we did not conduct formal tests for the lone grass-bush species, *A. pulchellus*,
310 inspecting its genetic correlation matrix (fig. 1, table A1) shows that this species displays some
311 similarities to trunk-ground lizards. In particular, this species had weak (and occasionally
312 negative) genetic correlations between the pelvis and all limb bones, similar to all trunk-ground
313 species. *A. pulchellus* also showed genetic correlations between hindlimb and forelimb bones that
314 were noticeably weaker than the other two species in the Puerto Rican lineage (fig. 1, table A1).

315

316

317

Discussion

318 Here we present two significant findings about the evolution of quantitative genetic architecture
319 within the adaptive radiation of West Indian *Anolis* lizards. First, when viewed in terms of its

320 effects on multivariate response to selection, we show that the overall structure of the *Anolis* **G**
321 matrix retains a phylogenetic signal. Although the seven species we studied have been separated
322 for 20–44 million years, all **G** matrices predicted a very similar multivariate evolutionary
323 response, and more closely related species had more similar **G** matrices. Second, despite this
324 phylogenetic signal in the overall structure of **G**, pairwise genetic correlations between limb traits
325 and body traits showed consistent signatures of convergence, suggesting that they have been
326 adaptively shaped by similar selection pressures resulting from each ecomorph's niche. In
327 particular, longer-limbed trunk-ground lizards show a decoupling of limb length and pelvis width
328 relative to shorter-limbed trunk-crown lizards, demonstrating that convergent changes in genetic
329 architecture may accompany repeated morphological adaptation. Taken together, our results
330 show that selection may alter **G** in predictable and evolutionarily consequential ways without
331 leading to major changes in its overall structure.

332 From the perspective of overall multivariate response to selection, **G** is remarkably
333 similar across the *Anolis* radiation, with predicted responses to selection in random directions
334 showing strong positive correlations ranging from .76 to .92. Over the span of a few generations,
335 then, morphological divergence of species with the **G** matrices estimated here should be
336 constrained to lie along directions defined by quantitative genetic architecture. Indeed, previous
337 work has shown that divergence of these species remains aligned with the major axis of genetic
338 variation, \mathbf{g}_{\max} , even after ~44 million years of divergence (McGlothlin et al. 2018).

339 The similarity of the overall structure of **G** declined with greater phylogenetic distance.
340 This pattern suggests that the overall structure of **G** changes relatively slowly, remaining
341 conserved over millions of years. While similarity of **G** in closely related species may in part
342 reflect comparable patterns of contemporary selection in species in the same lineage, most

343 similarity is likely attributable to shared evolutionary history. In addition to this phylogenetic
344 trend, we found that more distantly related species also show greater variance in random skewers
345 correlations. Although many distantly related species have dissimilar **G** matrices, some pairs
346 have highly congruent **G**, a pattern that is not explained by convergent morphology. This
347 increased variance emphasizes the unpredictability of the evolution of **G** structure over longer
348 timescales.

349 When considering more subtle changes in **G**—shifts in trait-specific genetic variances and
350 correlations—we found evidence that **G** can change repeatedly and predictably in response to
351 similar selection pressures. The strongest convergence occurred in genetic correlations between
352 limb bones and pelvis width, which were significantly reduced in trunk-ground species relative to
353 trunk-crown species. In some cases, genetic correlations differed in sign between ecomorphs.
354 When this was the case, genetic correlations were usually negative in trunk-ground species and
355 positive in trunk-crown species. These results indicate that the pattern of genetic integration was
356 subtly remodeled in the transition from trunk-crown to trunk-ground ecomorphs (or vice versa),
357 most notably in the relationship between limb length and pelvis width, for which trunk-ground
358 species showed weaker genetic correlations when compared to trunk-crown species.

359 The ecomorph difference in the genetic correlations between limb length and pelvis width
360 is likely to result from a combination of directional selection and correlational selection acting on
361 these traits. Ecomorph differences in limb length have clear links to performance within their
362 characteristic habitats (Losos and Sinervo 1989; Losos 1990; Irschick and Losos 1998),
363 suggesting that they have been driven apart by divergent directional selection. The longer
364 hindlimbs of trunk-ground lizards facilitate running faster on flatter surfaces, whereas the shorter
365 hindlimbs of trunk-crown lizards are suited for a wider variety of perches (Losos 1990; Losos and

366 Irschick 1996; Irschick and Losos 1998). Strong directional selection acting only on limb length
367 could reduce its genetic correlations with other traits; however, it is also likely that correlational
368 selection has played a role. The evolution of trunk-ground anoles from a hypothetical trunk-
369 crown ancestor would require evolution of longer legs without a concomitant increase in the
370 pelvis, which may lead to negative correlational selection to decouple the two traits. In contrast,
371 correlational selection might favor a positive correlation between the two traits in trunk-crown
372 anoles, perhaps because a matching limb and pelvic morphology would facilitate agility on
373 branches.

374 Differences in hindlimb length between trunk-crown and trunk-ground ecomorphs are
375 apparent at hatching and appear to emerge mostly via changes in developmental patterning early
376 in embryonic development rather than differences in growth (Sanger et al. 2012). The
377 developmental genetic networks underlying limb growth and development are well understood
378 (Rabinowitz and Vokes 2012), and comparative genomic evidence indicates that genes expressed
379 in these networks experienced enhanced positive selection during the radiation of anoles (Tollis
380 et al. 2018). Limb-development networks share some genes in common with the network
381 underlying development of the pelvic girdle (Sears et al. 2015). Therefore, it is likely that
382 changes in genetic correlations between limb length and pelvis involve evolutionary changes in
383 the expression of some of these shared genes. Future work should explore remodeling of these
384 networks to understand the developmental genetic underpinnings of convergent morphological
385 evolution in anoles.

386 Weaker genetic correlations between limbs and body traits likely facilitated the evolution
387 of longer hindlimbs in trunk-ground anoles without correlated changes in the rest of the body.
388 Such genetic decoupling of limbs and body may help explain the remarkable adaptability of the

389 trunk-ground ecomorph. Trunk-ground anoles seem to be especially capable of colonizing new
390 habitats. Trunk-ground species have successfully colonized the Bahamas and the Virgin Islands
391 (*A. sagrei* and *A. cristatellus*, respectively) and have become established invaders in a number of
392 locations following introduction by humans (Kolbe et al. 2004; Eales et al. 2008; Losos 2009).
393 Trunk-ground anoles also have greater species richness within islands (Losos 2009), in part
394 because they have radiated into ecologically distinct macrohabitats (Glor et al. 2003). Some of
395 this adaptability is likely due to rapid evolution in limb length, such as has been demonstrated in
396 experimental populations of *A. sagrei* (Losos et al. 1997, 2001; Kolbe et al. 2012). Although
397 comparable studies have not been conducted using trunk-crown ecomorphs, their stronger genetic
398 correlations between limb traits and body traits suggest that rapid, independent evolution of limb
399 length would not be as likely in trunk-crown species.

400 The genetic correlations between pelvis and limb length in the single grass-bush anole we
401 examined resemble those of trunk-ground anoles, suggesting either similar selection or common
402 ancestry, or a combination of the two. Grass-bush anoles have long hindlimbs relative to their
403 body width, suggesting that a combination of directional and correlational selection may have
404 reduced these correlations. However, *A. pulchellus* is likely to have evolved from a trunk-ground
405 ancestor (Poe et al. 2017), which suggests that both this species and the closely related *A.*
406 *cristatellus* may have inherited weakened genetic correlations between pelvis and limbs from a
407 common ancestor. In other respects, however, the genetic correlation structure of *A. pulchellus* is
408 dissimilar to that of *A. cristatellus*. In contrast to *A. cristatellus*, *A. pulchellus* appears to have
409 attained differences between the lengths of its hindlimbs and forelimbs via a reduction in the
410 genetic correlations between the two, a feature it shares with the distantly related trunk-ground
411 lizard *A. lineatopus*.

412

Conclusion

413 The evolution of **G** in West Indian anoles illustrates how the complex interplay between selection
414 and history influences genetic architecture. **G** reflects neither an irresistible pattern of constraint
415 nor an easily adapted phenotype responding quickly to environmental pressures. Patterns of
416 genetic covariation have potentially influenced the pathways that selection may follow, as
417 evidenced by evolution along a deeply conserved genetic line of least resistance in this radiation
418 (McGlothlin et al. 2018). At the same time, as we show here, selection leaves an imprint, if
419 subtle, upon **G** as species diverge. We did not observe a full-scale overhaul of **G** as ecomorphs
420 evolved. However, small-scale differences in the elements of **G** involving critical morphological
421 modules arose predictably between ecomorphs and may have had substantial evolutionary
422 consequences. Our results emphasize that while genetic constraints may change as adaptation
423 proceeds, these changes need not be large to facilitate phenotypic diversification. Rather, the
424 convergent changes we observed in the individual elements of **G**, particularly between the limbs
425 and the body, demonstrate that consistent selection pressures can alter underlying genetic
426 constraints in subtle ways that facilitate adaptation and influence future evolutionary potential.

427

428

429

Acknowledgments

430 We thank Simon Pearish and Michelle Sivilich for managing the lizard colony. Dozens of
431 undergraduates at the University of Virginia provided animal care and assistance with data
432 collection; special thanks is due to Margo Adler, Tyler Cassidy, Brian Duggar, Maridel
433 Fredericksen, Casey Furr, Jessie Handy, Bryan Hendrick, Uma Pendem, Jeff Wright, and

434 Elizabeth Zipperle, Leleña Avila, Chris Feldman, Vince Formica, Tonia Hsieh, Melissa Losos,
435 Ashli Moore, Liam Revell, and Matt Sanford assisted with field collections. We thank Brooke
436 Bodensteiner, Vincent Farallo, Kerry Gendreau, Angela Hornsby, and Josef Uyeda for comments
437 on the manuscript, and Luke Harmon, Gabriel Marroig, Emília Martins, and Liam Revell for
438 helpful discussions. This work was supported by the National Science Foundation (grant numbers
439 DEB 0519658 and 0650078 to E.D.B. III and DEB 0519777 and 0722475 to J.B.L.), University
440 of Virginia, and Virginia Tech. The authors declare that there are no conflicts of interest.

441

442

443

Statement of Authorship

444 J.B.L. and E.D.B. III conceived the study; J.W.M. and J.J.K. contributed to study design; J.W.M.,
445 J.J.K., J.B.L., and E.D.B. III performed field collections; J.W.M. and E.D.B. III oversaw the
446 breeding experiment; J.W.M., M.E.K., and H.V.W. collected data; J.W.M. analyzed data; J.W.M.
447 drafted the manuscript and all authors contributed to the final version of the manuscript.

448

449

450

Data and Code Availability

451 Raw data for estimating **G** matrices are available in a Dryad Data Repository from a previous
452 publication (<https://datadryad.org/stash/dataset/doi:10.5061/dryad.pt2g084>). All code and
453 processed data are available at <https://github.com/joelmcg/AnolisG> and will be archived in Dryad
454 upon manuscript acceptance.

455

456

Literature Cited

457 Agrawal, A. F., E. D. Brodie, III, and L. H. Rieseberg. 2001. Possible consequences of genes of

458 major effect: transient changes in the **G**-matrix. *Genetica* 112:33-43.

459 Aguirre, J. D., E. Hine, K. McGuigan, and M. W. Blows. 2014. Comparing **G**: multivariate

460 analysis of genetic variation in multiple populations. *Heredity* 112:21-29.

461 Arnold, S. J., R. Bürger, P. A. Hohenlohe, B. C. Ajie, and A. G. Jones. 2008. Understanding the

462 evolution and stability of the **G**-matrix. *Evolution* 62:2451-2461.

463 Arnold, S. J., M. E. Pfrender, and A. G. Jones. 2001. The adaptive landscape as a conceptual

464 bridge between micro- and macroevolution. *Genetica* 112-113:9-32.

465 Bégin, M., and D. A. Roff. 2003. The constancy of the **G** matrix through species divergence and

466 the effects of quantitative genetic constraints on phenotypic evolution: a case study in

467 crickets. *Evolution* 57:1107-1120.

468 —. 2004. From micro- to macroevolution through quantitative genetic variation: positive

469 evidence from field crickets. *Evolution* 58:2287-2304.

470 Beuttell, K., and J. B. Losos. 1999. Ecological morphology of Caribbean anoles. *Herpetological*

471 *Monographs*:1-28.

472 Björklund, M., A. Husby, and L. Gustafsson. 2013. Rapid and unpredictable changes of the **G**-

473 matrix in a natural bird population over 25 years. *Journal of Evolutionary Biology* 26:1-

474 13.

475 Blomberg, S. P., T. Garland, and A. R. Ives. 2003. Testing for phylogenetic signal in comparative

476 data: Behavioral traits are more labile. *Evolution* 57:717-745.

- 477 Blows, M. W., and A. A. Hoffmann. 2005. A reassessment of genetic limits to evolutionary
478 change. *Ecology* 86:1371-1384.
- 479 Bolstad, G. H., T. F. Hansen, C. Pelabon, M. Falahati-Anbaran, R. Perez-Barrales, and W. S.
480 Armbruster. 2014. Genetic constraints predict evolutionary divergence in *Dalechampia*
481 blossoms. *Philosophical Transactions of the Royal Society B-Biological Sciences* 369.
- 482 Brodie, E. D., III. 1989. Genetic correlations between morphology and antipredator behaviour in
483 natural populations of the garter snakes *Thamnophis ordinoides*. *Nature* 342:542-543.
- 484 —. 1992. Correlational selection for color pattern and antipredator behavior in the garter snake
485 *Thamnophis ordinoides*. *Evolution* 46:1284-1298.
- 486 Cano, J. M., A. Laurila, J. Palo, and J. Merilä. 2004. Population differentiation in **G** matrix
487 structure due to natural selection in *Rana temporaria*. *Evolution* 58:2013-2020.
- 488 Careau, V., M. E. Wolak, P. A. Carter, and T. Garland. 2015. Evolution of the additive genetic
489 variance-covariance matrix under continuous directional selection on a complex
490 behavioural phenotype. *Proceedings of the Royal Society B-Biological Sciences* 282.
- 491 Chenoweth, S. F., H. D. Rundle, and M. W. Blows. 2010. The contribution of selection and
492 genetic constraints to phenotypic divergence. *American Naturalist* 175:186-196.
- 493 Cheverud, J. M. 1984. Quantitative genetics and developmental constraints on evolution by
494 selection. *Journal of Theoretical Biology* 110:155-171.
- 495 —. 1988. A comparison of genetic and phenotypic correlations. *Evolution* 42:958-968.
- 496 Cheverud, J. M., and G. Marroig. 2007. Comparing covariance matrices: random skewers method
497 compared to the common principal components model. *Genetics and Molecular Biology*
498 30:461-469.

- 499 Cox, R. M., C. L. Cox, J. W. McGlothlin, D. C. Card, A. L. Andrew, and T. A. Castoe. 2017.
500 Hormonally mediated increases in sex-biased gene expression accompany the breakdown
501 of between-sex genetic correlations in a sexually dimorphic lizard. *American Naturalist*
502 189:315-332.
- 503 Delph, L. F., J. C. Steven, I. A. Anderson, C. R. Herlihy, and E. D. Brodie, III. 2011. Elimination
504 of a genetic correlation between the sexes via artificial correlational selection. *Evolution*
505 65:2872-2880.
- 506 Dobzhansky, T. 1937, *Genetics and the Origin of Species*, Columbia Univ. Press.
- 507 Doroszuk, A., M. W. Wojewodzic, G. Gort, and J. E. Kammenga. 2008. Rapid divergence of
508 genetic variance-covariance matrix within a natural population. *American Naturalist*
509 171:291-304.
- 510 Eales, J., R. S. Thorpe, and A. Malhotra. 2008. Weak founder effect signal in a recent
511 introduction of Caribbean *Anolis*. *Molecular Ecology* 17:1416-1426.
- 512 Eroukhmanoff, F., and E. I. Svensson. 2011. Evolution and stability of the **G**-matrix during the
513 colonization of a novel environment. *Journal of Evolutionary Biology* 24:1363-1373.
- 514 Falconer, D. S., and T. F. C. MacKay. 1996, *Introduction to Quantitative Genetics*. Harlow,
515 England, Prentice Hall.
- 516 Gilmour, A. R., B. J. Gogel, B. R. Cullis, and R. Thompson. 2009, *ASReml User Guide Release*
517 3.0. Hemel Hempstead, UK, VSN International Ltd.
- 518 Glor, R. E., J. J. Kolbe, R. Powell, A. Larson, and J. B. Losos. 2003. Phylogenetic analysis of
519 ecological and morphological diversification in Hispaniolan trunk-ground anoles (*Anolis*
520 *cybotes* group). *Evolution* 57:2383-2397.

- 521 Grant, P. R., and B. R. Grant. 1995. Predicting microevolutionary responses to directional
522 selection on heritable variation. *Evolution* 49:241-251.
- 523 Hadfield, J. D., A. Nutall, D. Osorio, and I. P. F. Owens. 2007. Testing the phenotypic gambit:
524 phenotypic, genetic and environmental correlations of colour. *Journal of Evolutionary*
525 *Biology* 20:549-557.
- 526 Hansen, T. F., and D. Houle. 2008. Measuring and comparing evolvability and constraint in
527 multivariate characters. *Journal of Evolutionary Biology* 21:1201-1219.
- 528 Harmon, L. J., and R. E. Glor. 2010. Poor statistical performance of the Mantel test in
529 phylogenetic comparative analyses. *Evolution* 64:2173-2178.
- 530 Harmon, L. J., J. J. Kolbe, J. M. Cheverud, and J. B. Losos. 2005. Convergence and the
531 multidimensional niche. *Evolution* 59:409-421.
- 532 Hine, E., S. F. Chenoweth, H. D. Rundle, and M. W. Blows. 2009. Characterizing the evolution
533 of genetic variance using genetic covariance tensors. *Philosophical Transactions of the*
534 *Royal Society B-Biological Sciences* 364:1567-1578.
- 535 Houle, D., G. H. Bolstad, K. van der Linde, and T. F. Hansen. 2017. Mutation predicts 40 million
536 years of fly wing evolution. *Nature* 548:447-+.
- 537 Houle, D., and K. Meyer. 2015. Estimating sampling error of evolutionary statistics based on
538 genetic covariance matrices using maximum likelihood. *Journal of Evolutionary Biology*
539 28:1542-1549.
- 540 Irschick, D. J., and J. B. Losos. 1998. A comparative analysis of the ecological significance of
541 maximal locomotor performance in Caribbean Anolis lizards. *Evolution* 52:219-226.

- 542 Jones, A. G., S. J. Arnold, and R. Bürger. 2003. Stability of the **G**-matrix in a population
543 experiencing pleiotropic mutation, stabilizing selection, and genetic drift. *Evolution*
544 57:1747-1760.
- 545 —. 2004. Evolution and stability of the **G**-matrix on a landscape with a moving optimum.
546 *Evolution* 58:1639-1654.
- 547 Jones, A. G., R. Bürger, and S. J. Arnold. 2014. Epistasis and natural selection shape the
548 mutational architecture of complex traits. *Nature Communications* 5.
- 549 Jones, A. G., R. Bürger, S. J. Arnold, P. A. Hohenlohe, and J. C. Uyeda. 2012. The effects of
550 stochastic and episodic movement of the optimum on the evolution of the **G**-matrix and
551 the response of the trait mean to selection. *Journal of Evolutionary Biology* 25:2210-
552 2231.
- 553 Kim, S. 2015. ppcor: An R package for a fast calculation to semi-partial correlation coefficients.
554 *Commun Stat Appl Methods* 22:665-674.
- 555 Kolbe, J. J., R. E. Glor, L. R. G. Schettino, A. C. Lara, A. Larson, and J. B. Losos. 2004. Genetic
556 variation increases during biological invasion by a Cuban lizard. *Nature* 431:177-181.
- 557 Kolbe, J. J., M. Leal, T. W. Schoener, D. A. Spiller, and J. B. Losos. 2012. Founder effects
558 persist despite adaptive differentiation: a field experiment with lizards. *Science* 335:1086-
559 1089.
- 560 Kolbe, J. J., L. J. Revell, B. Szekely, E. D. Brodie, and J. B. Losos. 2011. Convergent evolution
561 of phenotypic integration and Its alignment with morphological diversification in
562 Caribbean *Anolis* ecomorphs. *Evolution* 65:3608-3624.
- 563 Lande, R. 1979. Quantitative genetic analysis of multivariate evolution, applied to brain:body
564 size allometry. *Evolution* 33:402-416.

- 565 —. 1980. The genetic covariance between characters maintained by pleiotropic mutations.
566 *Genetics* 94:203-215.
- 567 Losos, J. B. 1990. Ecomorphology, performance capability, and scaling of West Indian *Anolis*
568 lizards: an evolutionary analysis. *Ecological Monographs* 60:369-388.
- 569 —. 1994. Integrative approaches to evolutionary ecology: *Anolis* lizards as model systems.
570 *Annual Review of Ecology and Systematics* 25:467-493.
- 571 —. 2009. *Lizards in an Evolutionary Tree: Ecology and Adaptive Radiation of Anoles*. Berkeley,
572 Univ. of California Press.
- 573 —. 2011. Convergence, adaptation, and constraint. *Evolution* 65:1827-1840.
- 574 Losos, J. B., and D. J. Irschick. 1996. The effect of perch diameter on escape behaviour of *Anolis*
575 lizards: laboratory predictions and field tests. *Animal Behaviour* 51:593-602.
- 576 Losos, J. B., T. R. Jackman, A. Larson, K. de Queiroz, and L. Rodríguez-Schettino. 1998.
577 Contingency and determinism in replicated adaptive radiations of island lizards. *Science*
578 279:2115-2118.
- 579 Losos, J. B., T. W. Schoener, K. I. Warheit, and D. Creer. 2001. Experimental studies of adaptive
580 differentiation in Bahamian *Anolis* lizards. *Genetica* 112:399-415.
- 581 Losos, J. B., and B. Sinervo. 1989. The effects of morphology and perch diameter on sprint
582 performance of *Anolis* lizards. *Journal of Experimental Biology* 145:23-30.
- 583 Losos, J. B., K. I. Warheit, and T. W. Schoener. 1997. Adaptive differentiation following
584 experimental island colonization in *Anolis* lizards. *Nature* 387:70-73.
- 585 Mahler, D. L., T. Ingram, L. J. Revell, and J. B. Losos. 2013. Exceptional convergence on the
586 macroevolutionary landscape in island lizard radiations. *Science* 341:292-295.

- 587 Marroig, G., and J. M. Cheverud. 2001. A comparison of phenotypic variation and covariation
588 patterns and the role of phylogeny. Ecology, and ontogeny during cranial evolution of
589 new world monkeys. *Evolution* 55:2576-2600.
- 590 Martins, E. P., and T. F. Hansen. 1997. Phylogenies and the comparative method: a general
591 approach to incorporating phylogenetic information into the analysis of interspecific data.
592 *American Naturalist* 149:646-667.
- 593 McGlothlin, J. W., M. E. Kobiela, H. V. Wright, D. L. Mahler, J. J. Kolbe, J. B. Losos, and E. D.
594 Brodie, III. 2018. Adaptive radiation along a deeply conserved genetic line of least
595 resistance in *Anolis* lizards. *Evolution Letters* 2:310-322.
- 596 McGlothlin, J. W., P. G. Parker, V. Nolan, Jr., and E. D. Ketterson. 2005. Correlational selection
597 leads to genetic integration of body size and an attractive plumage trait in dark-eyed
598 juncos. *Evolution* 59:658-671.
- 599 McGuigan, K. 2006. Studying phenotypic evolution using multivariate quantitative genetics.
600 *Molecular Ecology* 15:883-896.
- 601 McGuigan, K., S. F. Chenoweth, and M. W. Blows. 2005. Phenotypic divergence along lines of
602 genetic variance. *American Naturalist* 165:32-43.
- 603 Melo, D., G. Garcia, A. Hubbe, A. P. Assis, and G. Marroig. 2015. EvolQG - An R package for
604 evolutionary quantitative genetics. *F1000Res* 4:925.
- 605 Merilä, J., and M. Björklund. 2004. Phenotypic integration as a constraint and adaptation, Pages
606 107-129 in M. Pigliucci, and K. Preston, eds. *Phenotypic Integration: Studying the*
607 *Ecology and Evolution of Complex Phenotypes*. Oxford, Oxford Univ. Press.
- 608 Paradis, E., J. Claude, and K. Strimmer. 2004. APE: Analyses of Phylogenetics and Evolution in
609 R language. *Bioinformatics* 20:289-290.

- 610 Phillips, P. C., and S. J. Arnold. 1989. Visualizing multivariate selection. *Evolution* 43:1209-
611 1222.
- 612 Poe, S., A. Nieto-Montes de Oca, O. Torres-Carvajal, K. de Queiroz, J. A. Velasco, B. Truett, L.
613 N. Gray et al. 2017. A phylogenetic, biogeographic, and taxonomic study of all extant
614 species of *Anolis* (Squamata; Iguanidae). *Systematic Biology* 66:663-697.
- 615 R Core Team. 2019. R: A language and environment for statistical computing. . Vienna, Austria,
616 R Foundation for Statistical Computing.
- 617 Rabinowitz, A. H., and S. A. Vokes. 2012. Integration of the transcriptional networks regulating
618 limb morphogenesis. *Developmental Biology* 368:165-180.
- 619 Revell, L. J. 2007. The **G** matrix under fluctuating correlational mutation and selection.
620 *Evolution* 61:1857-1872.
- 621 —. 2012. phytools: an R package for phylogenetic comparative biology (and other things).
622 *Methods in Ecology and Evolution* 3:217-223.
- 623 Revell, L. J., D. L. Mahler, J. R. Sweeney, M. Sobotka, V. E. Fancher, and J. B. Losos. 2010.
624 Nonlinear selection and the evolution of variances and covariances for continuous
625 characters in an anole. *Journal of Evolutionary Biology* 23:407-421.
- 626 Roff, D. A. 1997, *Evolutionary Quantitative Genetics*. New York, Chapman & Hall.
- 627 Roff, D. A., and D. J. Fairbairn. 2012. A test of the hypothesis that correlational selection
628 generates genetic correlations. *Evolution* 66:2953-2960.
- 629 Sanger, T. J., L. J. Revell, J. J. Gibson-Brown, and J. B. Losos. 2012. Repeated modification of
630 early limb morphogenesis programmes underlies the convergence of relative limb length
631 in *Anolis* lizards. *Proceedings of the Royal Society B-Biological Sciences* 279:739-748.

- 632 Schluter, D. 1996. Adaptive radiation along genetic lines of least resistance. *Evolution* 50:1766-
633 1774.
- 634 Sears, K. E., T. D. Capellini, and R. Diogo. 2015. On the serial homology of the pectoral and
635 pelvic girdles of tetrapods. *Evolution* 69:2543-2555.
- 636 Stepan, S. J., P. C. Phillips, and D. Houle. 2002. Comparative quantitative genetics: evolution of
637 the **G** matrix. *Trends in Ecology & Evolution* 17:320-327.
- 638 Steven, J. C., I. A. Anderson, E. D. Brodie III, and L. F. Delph. 2020. Rapid reversal of a
639 potentially constraining genetic covariance between leaf and flower traits in *Silene*
640 *latifolia*. *Ecol Evol* 10:569-578.
- 641 Tollis, M., E. D. Hutchins, J. Stapley, S. M. Rupp, W. L. Eckalbar, I. Maayan, E. Lasku et al.
642 2018. Comparative genomics reveals accelerated evolution in conserved pathways during
643 the diversification of anole lizards. *Genome Biology and Evolution* 10:489-506.
- 644 Turelli, M. 1988. Phenotypic evolution, constant covariances, and the maintenance of additive
645 variance. *Evolution* 42:1342-1347.
- 646 Walsh, B., and M. W. Blows. 2009. Abundant genetic variation plus strong selection =
647 multivariate genetic constraints: a geometric view of adaptation. *Annual Review of*
648 *Ecology Evolution and Systematics* 40:41-59.
- 649 Walter, G. M., J. D. Aguirre, M. W. Blows, and D. Ortiz-Barrientos. 2018. Evolution of genetic
650 variance during adaptive radiation. *American Naturalist* 191:E108-E128.
- 651 Williams, E. E. 1972. The origin of faunas. Evolution of lizard congeners in a complex island
652 fauna: a trial analysis. *Evolutionary Biology* 6:47-89.
- 653 Wood, S. 2012. mgcv: Mixed GAM Computation Vehicle with GCV/AIC/REML smoothness
654 estimation.

655 Zheng, Y. C., and J. J. Wiens. 2016. Combining phylogenomic and supermatrix approaches, and
656 a time-calibrated phylogeny for squamate reptiles (lizards and snakes) based on 52 genes
657 and 4162 species. *Molecular Phylogenetics and Evolution* 94:537-547.

Appendix

Supplemental Tables

Table A1: **G** matrices and matrices of heritabilities (h^2 , diagonal) and genetic correlations (r_g , off-diagonal) for seven *Anolis* species. Approximate standard errors for are shown below each matrix. **G** matrices and standard errors are reprinted from McGlothlin et al. (2018). Although we did not conduct formal likelihood-ratio tests, parameters that exceeded their standard errors by a factor of two are shown in bold, which provides a guide to statistical significance. Traits are abbreviated as follows: JL = jaw length, HW = head width, PECT = pectoral width, PELV = pelvic width, HUM = humerus, UL = ulna, FEM = femur, and TIB = tibia. All traits were natural-log transformed and size-corrected for analysis.

Anolis cristatellus (Trunk-ground, Puerto Rico)

G ($\times 10^{-3}$)

	JL	HW	PECT	PELV	HUM	UL	FEM	TIB
JL	.329							
HW	.094	.449						
PECT	-.083	.349	1.426					
PELV	-.089	.240	.487	.546				
HUM	.293	.071	-.371	-.168	1.441			
UL	.079	.075	-.098	.017	1.008	1.087		
FEM	.208	.030	-.053	-.051	.904	.731	.809	
TIB	.268	.009	-.172	-.081	.945	.780	.783	.949

SE ($\times 10^{-3}$)

	JL	HW	PECT	PELV	HUM	UL	FEM	TIB
JL	.052							
HW	.029	.048						
PECT	.053	.066	.170					
PELV	.056	.049	.093	.113				
HUM	.057	.067	.128	.090	.200			
UL	.053	.063	.119	.087	.144	.175		
FEM	.035	.042	.077	.058	.093	.085	.071	
TIB	.037	.043	.081	.060	.096	.089	.067	.076

Anolis cristatellus (continued)

h^2/r_g

	JL	HW	PECT	PELV	HUM	UL	FEM	TIB
JL	.458							
HW	.245	.353						
PECT	-.122	.435	.306					
PELV	-.210	.484	.552	.196				
HUM	.425	.088	-.259	-.190	.231			
UL	.132	.108	-.078	.022	.805	.185		
FEM	.403	.049	-.049	-.076	.837	.779	.482	
TIB	.480	.014	-.148	-.113	.808	.768	.894	.561

h^2/r_g SE

	JL	HW	PECT	PELV	HUM	UL	FEM	TIB
JL	.057							
HW	.068	.028						
PECT	.079	.073	.029					
PELV	.130	.093	.092	.037				
HUM	.081	.082	.084	.101	.028			
UL	.091	.090	.094	.111	.057	.027		
FEM	.066	.068	.072	.087	.049	.058	.025	
TIB	.063	.066	.069	.085	.051	.057	.017	.023

Anolis evermanni (Trunk-crown, Puerto Rico)

G ($\times 10^{-3}$)

	JL	HW	PECT	PELV	HUM	UL	FEM	TIB
JL	.251							
HW	-.013	.314						
PECT	.016	.411	1.062					
PELV	-.017	.183	.435	.623				
HUM	.143	.022	.051	.139	.866			
UL	.141	-.026	.097	.145	.884	.971		
FEM	.070	.040	.228	.279	.850	.922	1.224	
TIB	.121	.047	.178	.258	.971	1.064	1.427	1.751

SE ($\times 10^{-3}$)

	JL	HW	PECT	PELV	HUM	UL	FEM	TIB
JL	.029							
HW	.027	.049						
PECT	.048	.069	.163					
PELV	.040	.054	.099	.146				
HUM	.049	.061	.110	.091	.160			
UL	.049	.062	.113	.093	.135	.156		
FEM	.041	.054	.098	.083	.108	.110	.117	
TIB	.048	.064	.114	.097	.124	.128	.125	.174

h^2/r_g

	JL	HW	PECT	PELV	HUM	UL	FEM	TIB
JL	.415							
HW	-.047	.244						
PECT	.031	.712	.280					
PELV	-.043	.414	.535	.227				
HUM	.306	.042	.053	.189	.194			
UL	.286	-.046	.096	.186	.964	.212		
FEM	.126	.064	.200	.319	.825	.846	.599	
TIB	.182	.064	.131	.247	.788	.816	.975	.704

h^2/r_g SE

	JL	HW	PECT	PELV	HUM	UL	FEM	TIB
JL	.033							
HW	.097	.032						
PECT	.094	.077	.035					
PELV	.101	.108	.106	.048				
HUM	.096	.117	.117	.122	.032			
UL	.092	.113	.111	.117	.044	.029		
FEM	.072	.087	.083	.089	.066	.053	.030	
TIB	.069	.085	.083	.089	.071	.057	.011	.034

Anolis grahami (Trunk-crown, Jamaica)

G ($\times 10^{-3}$)

	JL	HW	PECT	PELV	HUM	UL	FEM	TIB
JL	.246							
HW	.218	.296						
PECT	.127	.122	.351					
PELV	.193	.126	.173	.704				
HUM	.152	.067	.167	.264	1.003			
UL	.129	.131	.122	.130	.856	1.171		
FEM	.126	-.005	.081	.186	.625	.559	.510	
TIB	.146	.034	.171	.269	.732	.724	.549	.648

SE ($\times 10^{-3}$)

	JL	HW	PECT	PELV	HUM	UL	FEM	TIB
JL	.049							
HW	.051	.082						
PECT	.064	.081	.151					
PELV	.068	.084	.113	.169				
HUM	.140	.186	.238	.176	.465			
UL	.103	.133	.177	.186	.323	.405		
FEM	.052	.099	.139	.111	.230	.191	.170	
TIB	.056	.102	.145	.104	.230	.181	.163	.179

h^2/r_g

	JL	HW	PECT	PELV	HUM	UL	FEM	TIB
JL	.421							
HW	.807	.240						
PECT	.434	.377	.133					
PELV	.465	.277	.349	.277				
HUM	.307	.123	.281	.315	.168			
UL	.240	.222	.191	.143	.790	.159		
FEM	.355	-.013	.191	.311	.873	.723	.453	
TIB	.367	.076	.358	.399	.908	.831	.955	.544

h^2/r_g SE

	JL	HW	PECT	PELV	HUM	UL	FEM	TIB
JL	.056							
HW	.092	.056						
PECT	.190	.229	.054					
PELV	.134	.173	.210	.054				
HUM	.266	.341	.392	.192	.072			
UL	.188	.221	.281	.199	.155	.050		
FEM	.136	.249	.323	.171	.165	.160	.122	
TIB	.127	.231	.289	.134	.165	.124	.037	.110

Anolis lineatopus (Trunk-ground, Jamaica)

G ($\times 10^{-3}$)

	JL	HW	PECT	PELV	HUM	UL	FEM	TIB
JL	.442							
HW	.286	.263						
PECT	.385	.290	.750					
PELV	.193	.132	.343	.916				
HUM	.321	.240	.223	-.016	.968			
UL	.412	.297	.308	-.200	.942	1.047		
FEM	.423	.180	.547	.228	.530	.540	1.013	
TIB	.368	.145	.528	.182	.464	.495	.864	.825

SE ($\times 10^{-3}$)

	JL	HW	PECT	PELV	HUM	UL	FEM	TIB
JL	.103							
HW	.059	.090						
PECT	.101	.100	.309					
PELV	.158	.139	.254	.352				
HUM	.127	.103	.213	.200	.291			
UL	.106	.104	.186	.174	.240	.270		
FEM	.168	.130	.233	.256	.255	.248	.346	
TIB	.147	.117	.212	.227	.226	.222	.295	.272

h^2/r_g

	JL	HW	PECT	PELV	HUM	UL	FEM	TIB
JL	.536							
HW	.837	.177						
PECT	.668	.652	.151					
PELV	.303	.269	.414	.253				
HUM	.491	.475	.262	-.017	.161			
UL	.605	.566	.348	-.204	.936	.169		
FEM	.633	.349	.627	.237	.535	.525	.645	
TIB	.610	.311	.672	.209	.519	.533	.945	.587

h^2/r_g SE

	JL	HW	PECT	PELV	HUM	UL	FEM	TIB
JL	.089							
HW	.114	.056						
PECT	.158	.206	.059					
PELV	.217	.265	.263	.087				
HUM	.167	.196	.251	.223	.044			
UL	.118	.178	.223	.177	.071	.040		
FEM	.143	.237	.202	.232	.201	.196	.155	
TIB	.146	.238	.188	.233	.206	.196	.029	.143

Anolis pulchellus (Grass-bush, Puerto Rico)

G ($\times 10^{-3}$)

	JL	HW	PECT	PELV	HUM	UL	FEM	TIB
JL	.084							
HW	.080	.157						
PECT	.222	.215	.895					
PELV	.070	.065	.300	.766				
HUM	.148	.040	.153	-.036	.745			
UL	.180	.080	.214	-.152	.773	.982		
FEM	.092	.040	.156	.126	.475	.524	.701	
TIB	.089	.030	.136	.134	.403	.524	.648	.723

SE ($\times 10^{-3}$)

	JL	HW	PECT	PELV	HUM	UL	FEM	TIB
JL	.050							
HW	.040	.059						
PECT	.075	.070	.268					
PELV	.066	.061	.192	.244				
HUM	.072	.068	.163	.127	.204			
UL	.082	.076	.155	.145	.197	.254		
FEM	.054	.053	.110	.083	.133	.118	.156	
TIB	.054	.045	.087	.082	.141	.143	.148	.168

h^2/r_g

	JL	HW	PECT	PELV	HUM	UL	FEM	TIB
JL	.076							
HW	.701	.124						
PECT	.810	.574	.211					
PELV	.276	.187	.363	.184				
HUM	.594	.118	.188	-.047	.106			
UL	.629	.204	.228	-.175	.905	.116		
FEM	.382	.122	.196	.172	.658	.632	.420	
TIB	.362	.090	.170	.181	.549	.622	.911	.476

h^2/r_g SE

	JL	HW	PECT	PELV	HUM	UL	FEM	TIB
JL	.044							
HW	.218	.044						
PECT	.237	.153	.057					
PELV	.259	.176	.191	.054				
HUM	.299	.201	.196	.167	.027			
UL	.295	.192	.164	.160	.066	.028		
FEM	.211	.158	.134	.113	.127	.113	.074	
TIB	.214	.134	.108	.112	.159	.130	.038	.086

Anolis sagrei (Trunk-ground, Bahamas)

G ($\times 10^{-3}$)

	JL	HW	PECT	PELV	HUM	UL	FEM	TIB
JL	.292							
HW	.112	.302						
PECT	-.002	.166	.286					
PELV	-.077	-.018	.035	.463				
HUM	.156	-.073	.027	-.109	.603			
UL	.027	-.142	-.047	.082	.462	.646		
FEM	.192	-.033	-.027	-.011	.409	.315	.368	
TIB	.177	-.111	-.036	-.003	.527	.507	.434	.606

SE ($\times 10^{-3}$)

	JL	HW	PECT	PELV	HUM	UL	FEM	TIB
JL	.023							
HW	.021	.033						
PECT	.024	.030	.048					
PELV	.050	.055	.043	.073				
HUM	.035	.050	.050	.068	.092			
UL	.037	.044	.053	.062	.080	.116		
FEM	.024	.037	.042	.041	.051	.051	.054	
TIB	.026	.044	.051	.042	.058	.061	.056	.073

h^2/r_g

	JL	HW	PECT	PELV	HUM	UL	FEM	TIB
JL	.469							
HW	.377	.269						
PECT	-.007	.566	.127					
PELV	-.211	-.049	.095	.147				
HUM	.372	-.171	.065	-.206	.133			
UL	.063	-.321	-.110	.149	.740	.130		
FEM	.585	-.100	-.085	-.027	.869	.647	.270	
TIB	.421	-.259	-.087	-.006	.873	.811	.919	.449

h^2/r_g SE

	JL	HW	PECT	PELV	HUM	UL	FEM	TIB
JL	.023							
HW	.059	.024						
PECT	.087	.083	.020					
PELV	.134	.146	.114	.021				
HUM	.077	.116	.118	.126	.019			
UL	.084	.097	.123	.112	.069	.022		
FEM	.059	.112	.131	.097	.055	.083	.034	
TIB	.054	.097	.122	.084	.048	.060	.026	.041

Anolis smaragdinus (Trunk-crown, Bahamas)

G ($\times 10^{-3}$)

	JL	HW	PECT	PELV	HUM	UL	FEM	TIB
JL	.348							
HW	.054	.161						
PECT	.251	.065	.830					
PELV	.102	-.002	.442	.560				
HUM	.268	.151	.130	.122	.395			
UL	.238	.094	.249	.300	.331	.452		
FEM	.205	.061	.136	.115	.285	.287	.344	
TIB	.296	.008	.221	.278	.351	.423	.420	.609

SE ($\times 10^{-3}$)

	JL	HW	PECT	PELV	HUM	UL	FEM	TIB
JL	.129							
HW	.091	.139						
PECT	.171	.174	.413					
PELV	.072	.068	.144	.142				
HUM	.130	.093	.163	.122	.280			
UL	.098	.134	.176	.175	.181	.286		
FEM	.114	.085	.184	.127	.149	.149	.165	
TIB	.125	.072	.205	.141	.120	.132	.158	.197

h^2/r_g

	JL	HW	PECT	PELV	HUM	UL	FEM	TIB
JL	.455							
HW	.227	.121						
PECT	.468	.176	.254					
PELV	.230	-.007	.648	.251				
HUM	.722	.600	.228	.259	.100			
UL	.601	.348	.406	.596	.783	.090		
FEM	.592	.257	.255	.262	.773	.728	.283	
TIB	.644	.025	.311	.477	.717	.806	.919	.454

h^2/r_g SE

	JL	HW	PECT	PELV	HUM	UL	FEM	TIB
JL	.137							
HW	.353	.101						
PECT	.248	.450	.116					
PELV	.151	.254	.179	.053				
HUM	.298	.421	.302	.261	.068			
UL	.235	.481	.296	.306	.290	.055		
FEM	.207	.348	.337	.274	.307	.311	.122	
TIB	.154	.223	.279	.205	.269	.243	.094	.118

Table A2: Random skewers correlations (r_{RS}) for each species pair. Point estimates, REML-MVN estimates, and 95% confidence intervals are shown. Point estimates occasionally lie outside the REML-MVN confidence interval because incorporating estimation error from two **G** matrices lead to negatively skewed distributions.

species 1	species 2	r_{RS}	REML-MVN	r_{RS}	2.5%	97.5%
CRIS	EVER	.89		.86	.80	.91
CRIS	GRAH	.84		.74	.59	.84
CRIS	LINE	.78		.70	.55	.81
CRIS	PULC	.87		.81	.71	.88
CRIS	SAGR	.88		.85	.79	.89
CRIS	SMAR	.81		.66	.43	.82
EVER	GRAH	.83		.74	.60	.84
EVER	LINE	.81		.73	.55	.83
EVER	PULC	.90		.84	.74	.91
EVER	SAGR	.84		.81	.75	.87
EVER	SMAR	.82		.68	.47	.81
GRAH	LINE	.85		.70	.52	.83
GRAH	PULC	.88		.75	.60	.86
GRAH	SAGR	.87		.76	.62	.86
GRAH	SMAR	.79		.61	.38	.77
LINE	PULC	.92		.79	.64	.89
LINE	SAGR	.76		.67	.52	.78
LINE	SMAR	.81		.63	.39	.79
PULC	SAGR	.82		.76	.66	.83
PULC	SMAR	.84		.66	.44	.82
SAGR	SMAR	.76		.63	.42	.77

Table A3: Estimates of phylogenetic signal (Blomberg's K) for all genetic variances and correlations. Point estimates, REML-MVN estimates, and 95% confidence intervals are shown. All estimates of K were significantly different from 0 and indistinguishable from 1.

Variations

Trait	K	REML-MVN K	2.5%	97.5%
JL	.81	.86	.65	1.11
HW	.69	.77	.61	1.05
PECT	1.16	1.13	.79	1.53
PELV	.90	.90	.69	1.18
RAD	.87	.90	.69	1.20
UL	1.15	1.03	.77	1.31
FEM	.99	1.00	.83	1.31
TIB	.90	.91	.77	1.13

Correlations

Trait 1	Trait 2	K	REML-MVN K	2.5%	97.5%
JL	HW	.92	.96	.74	1.26
JL	PECT	.71	.76	.64	1.00
JL	PELV	.88	.91	.67	1.25
JL	HUM	.91	.93	.69	1.20
JL	UL	.78	.84	.67	1.12
JL	FEM	1.04	1.00	.73	1.32
JL	TIB	.95	.92	.73	1.17
HW	PECT	.97	.97	.74	1.19
HW	PELV	1.04	1.01	.71	1.39
HW	HUM	1.04	1.01	.82	1.20
HW	UL	.97	.99	.84	1.14
HW	FEM	.91	.97	.78	1.20
HW	TIB	.97	.97	.82	1.16
PECT	PELV	1.02	.98	.74	1.30
PECT	HUM	.85	.92	.65	1.30
PECT	UL	.92	.94	.71	1.19
PECT	FEM	.91	.95	.77	1.18
PECT	TIB	1.02	1.01	.80	1.24
PELV	HUM	.90	.92	.75	1.15
PELV	UL	1.03	1.00	.77	1.19
PELV	FEM	.81	.89	.71	1.11
PELV	TIB	.93	.94	.72	1.18
HUM	UL	.90	.99	.76	1.22
HUM	FEM	.78	.92	.72	1.17
HUM	TIB	.76	.87	.71	1.13
UL	FEM	.87	.98	.71	1.31
UL	TIB	.80	.91	.71	1.17
FEM	TIB	.79	.93	.72	1.14

Table A4: Ecomorph effects given as evolutionary correlations (r_e) for all genetic variances and correlations. A positive value indicates that trunk-ground species have a higher value than trunk-crown species. Point estimates, REML-MVN estimates, and 95% confidence intervals are shown. Significant values are indicated with boldface.

Variations

Trait	r_e	REML-MVN r_e	2.5%	97.5%
JL	.62	.48	-.17	.88
HW	.52	.39	-.26	.84
PECT	.23	.19	-.27	.56
PELV	.03	-.04	-.85	.58
RAD	.44	.36	-.24	.78
UL	.09	.08	-.59	.70
FEM	.01	-.02	-.49	.34
TIB	-.35	-.34	-.65	.02

Correlations

Trait 1	Trait 2	r_e	REML-MVN r_e	2.5%	97.5%
JL	HW	.28	.25	-.13	.52
JL	PECT	-.23	-.21	-.60	.22
JL	PELV	-.56	-.49	-.84	-.03
JL	HUM	.09	.07	-.64	.79
JL	UL	-.20	-.17	-.64	.32
JL	FEM	.63	.55	.05	.90
JL	TIB	.49	.43	-.06	.84
HW	PECT	.24	.11	-.73	.57
HW	PELV	.03	.02	-.60	.58
HW	HUM	-.13	-.09	-.63	.52
HW	UL	-.01	.00	-.47	.50
HW	FEM	.08	.04	-.68	.64
HW	TIB	-.07	-.09	-.75	.48
PECT	PELV	-.37	-.27	-.79	.36
PECT	HUM	-.55	-.35	-.86	.39
PECT	UL	-.44	-.33	-.85	.35
PECT	FEM	-.11	-.10	-.70	.42
PECT	TIB	-.24	-.21	-.68	.28
PELV	HUM	-.96	-.78	-.98	-.32
PELV	UL	-.68	-.58	-.89	-.06
PELV	FEM	-.82	-.62	-.97	-.01
PELV	TIB	-.87	-.74	-.97	-.25
HUM	UL	-.16	-.14	-.82	.46
HUM	FEM	-.37	-.21	-.72	.59
HUM	TIB	-.33	-.21	-.70	.59
UL	FEM	-.64	-.35	-.86	.41
UL	TIB	-.58	-.37	-.82	.45
FEM	TIB	-.65	-.45	-.94	.20